Electrospun fixed dose formulations of amlodipine besylate and valsartan

Haitham Bukhary, Gareth R. Williams,* and Mine Orlu*

UCL School of Pharmacy, University College London, 29-39 Brunswick Square, London, WC1N 1AX, UK

* authors for correspondence. Email: g.williams@ucl.ac.uk (GRW); m.orlu@ucl.ac.uk (MO). Tel: +44 (0) 207 753 5868 (GRW); +44 (0) 207 753 5968 (MO).

Abstract

Increasing numbers of elderly people require multi-drug therapies. One route to improve adherence rates is to prepare fixed dose combinations (FDCs), in which multiple active ingredients are loaded into a single formulation. Here, we report the use of electrospinning to prepare fast-dissolving oral FDCs containing amlodipine besylate and valsartan, two drugs prescribed as FDCs for the treatment of hypertension. Electrospun fibers were prepared loaded with one or both drugs, using polyvinylpyrrolidone as the polymer matrix. The fibers were cylindrical in morphology and comprise amorphous solid dispersions except with the highest loadings of amlodipine besylate. HPLC demonstrated drug entrapment efficiencies of between 90 and 99% of the theoretical dose. The mats have folding endurances and thicknesses suitable for use as oral films. The amlodipine besylate-loaded systems are fast-dissolving, with 100% release obtained within 120 s. In contrast, valsartan release from its single-drug formulations took longer, ranging from 360 s to 24 min. With the FDC formulations, rapid release within 360 s was achieved when the loading was 5% w/w of each drug, but again the release time increased with drug loading. Electrospun fibers therefore have significant promise as FDCs, but the target drug and its loading need to be carefully considered.

Keywords: Fixed dose combinations, electrospinning, polyvinylpyrrolidone, amlodipine besylate, valsartan, fast dissolving films.

1. Introduction

In the UK, older people make up 20% of the population and consume almost 50% of prescription drugs (Gorard, 2006). The majority of people aged 65 and older are diagnosed with multiple diseases that require management with several active ingredients simultaneously, often to the extent of polypharmacy, which is loosely defined as synchronous use of two to five or more medicines (Fulton and Allen, 2005). The adherence of patients to their drug regimen is crucial for successful therapeutic outcomes (Jimmy and Jose, 2011), and patients involved in polypharmacy are likely to find it challenging to take all their medicines at the appropriate times. This can profoundly affect the patient's quality of life, and also adds extra economic costs for healthcare providers (Hughes, 2004). Therefore, it is the task of formulators to prepare medicines to minimize the burden on patients and maximize the likelihood of a dosage regimen being accurately followed.

Much work has been devoted to ensuring formulations have good patient acceptability (Liu et al., 2014), for instance to ensure ease of swallowing: this is key in designing geriatric oral formulations, in order to prevent oesophageal retention and risk of aspiration (Liu et al., 2014). An attractive solution to overcome the acceptability challenge is simplifying the treatment regimen for multiple drugs, by combining them in a single dosage form. Fixed dose combination (FDC) drug products are defined as those which combine two or more active pharmaceutical ingredients (APIs) in a single dosage form at a fixed dose ratio. FDCs are designed to facilitate simpler treatment plans for multiple drugs which have similarly timed regimens (Bangalore et al., 2007), and thereby improve patient compliance (European Medicines Agency, 2017). FDCs are expected to have particular promise for patients suffering from chronic conditions like hypertension and diabetes, where long term medication is required (Desai et al., 2013). It has been suggested that a 26% reduction in older patient non-adherence should be achievable using FDCs (Bangalore et al., 2007). However, FDC tablets or capsules tend to be larger than the individual drug formulations, and thus if poorly designed FDCs could in fact reduce patient compliance because of swallowing difficulties (European Medicines Agency, 2017).

A number of conventional pharmaceutical technologies have been used for commercial FDC product manufacturing (Desai et al., 2013), such as the incorporation of multiple drugs in separate layers of multilayer tablets (Mitra and Wu, 2012). Emerging technologies have also been investigated: for instance, 3D printing has been employed to produce a polypill containing five different APIs (Khaled et al., 2015). An alternative which has to date not been widely explored in the context of FDCs is electrospinning. This is a simple technique in which electrical energy is applied to a polymer/drug solution, usually resulting in amorphous solid dispersions (ASDs) in the form of nanoscale fibers. The production of ASDs can lead to enhanced dissolution and solubility, attractive for preparing formulations of APIs with low water solubility (Williams et al., 2012; Zamani et al., 2013). A range of polymers can be processed, and multiple active pharmaceutical ingredients incorporated into a single fiber formulation (Illangakoon et al., 2014; Li et al., 2013a).

As a result, electrospinning has been widely explored as a method for fabricating fast dissolving thin films (Williams et al., 2012). For example, an oral fast-dissolving drug delivery system was prepared from the hydrophilic polymer polyvinylpyrrolidone (PVP) and ibuprofen, and complete release of the drug observed in 10 s (Yu et al., 2009). Other fast-dissolving drug-loaded PVP fibres have been reported containing a wide variety of active ingredients, including ketoprofen (a non-steroidal anti-inflammatory drug) (Yu et al., 2010), irbesartan (used to treat high blood pressure) (Adeli, 2015), vitamin D (Li et al., 2013b), or isosorbide dinitrate (used in the treatment of angina),(Chen et al., 2016). Very rapid release can be achieved with multiple APIs in the same fiber formulation, as has been seen for electrospun polyvinylalcohol fibers loaded with caffeine and riboflavin (Li et al., 2013a) and PVP fibers containing paracetamol and caffeine (Illangakoon et al., 2014).

Fast-dissolving oral drug delivery systems have the advantage of immediate disintegration and drug dissolution occurring in the mouth, providing rapid onset of action (Seager, 1998). Since the formulation does not need to be taken with water, they can be used for patients suffering from dysphagia, common in the elderly. Sufficiently high aqueous solubility is crucial for their success, however. This requirement

becomes increasingly problematic with the increasing number of poorly water soluble drugs emerging onto the market (Nagy et al., 2010).

Amlodipine besylate and valsartan are frequently prescribed in combination as blood pressure lowering agents for the treatment of hypertension when monotherapy is not sufficient (Plosker and Robinson, 2008). An FDC (EXFORGE®) is available in the form of film coated tablets containing amlodipine besylate and valsartan in doses of 5/80 mg, 5/160 mg, and 10/160 mg. Both drugs have low aqueous solubility, and hence a fast-dissolving oral formulation would be highly valuable.

The aim of this project was to investigate the use of electrospinning to prepare FDCs of valsartan and amlodipine besylate, with the intended application as oral fast dissolving films. A series of single-drug and dual-drug loaded systems were prepared and fully characterized, and their disintegration and drug release evaluated.

2. Experimental details

2.1 Materials

Polyvinylpyrrolidone (PVP; MW 360,000 Da) and amlodipine besylate (AB) were purchased from Sigma-Aldrich, UK. Valsartan (VAL) was sourced from LKT Laboratories Inc., USA. Analytical grade ethanol, acetonitrile and methanol were procured from Sigma-Aldrich, UK. Deionised water was used for all studies, and all other chemicals used were of analytical grade.

2.2 Preparation of spinning solutions

10% w/v PVP solutions were prepared in ethanol, with stirring overnight to ensure complete dissolution. Drug-loaded solutions were prepared as detailed in Table 1, by pre-dissolving the required amount of AB or/and VAL in 2 mL of ethanol, then combining this with 5 mL of the PVP solution. Mechanical stirring was applied at room temperature for 20 min until homogeneous solutions were formed. Drug/polymer physical mixtures (PM) were prepared for control purposes.

Table 1. The compositions of the spinning solutions.

	ID	Drug loading (% w/w)	Drug mass in 2 mL ethanol (mg)	
			AB	VAL
AB formulations	A1	5	26	-
	A2	15	88	-
	A3	30	214	-
	A4	55	611	-
VAL formulations	V1	5	-	26
	V2	15	-	88
	V3	30	-	214
	V4	55	-	611
FDCs	AV1	5 / 5 AB / VAL	28.5	28.5
	AV2	15 / 15 AB / VAL	107	107
	AV3	30 / 30 AB / VAL	375	375

2.3 Electrospinning

Polymer solutions were loaded into 5 mL plastic syringes (Terumo, MediSupplies, UK) fitted with stainless steel dispensing needles (20G, 0.61 mm inner diameter, Nordson EFD, UK) with care taken to avoid any air bubbles. A voltage of +15 kV was applied to the needle (spinneret) using a HCP 35-35000 power supply (FuG Elektronik GmbH, Germany). The feed rate of the solution was controlled with a syringe pump (KDS100, Cole Parmer, UK) at 1.3 mL h^{-1}, and 5 mL of fluid was dispensed. The fibers were collected on a flat grounded collector (20 x 30 cm) covered with aluminum foil and situated 12 cm from the spinneret tip. Electrospinning was carried out under ambient conditions (18 – 23 °C and relative humidity of 26 – 63%). After fabrication, the electrospun fiber mats were stored in a vacuum desiccator over silica gel beads to aid evaporation of the remaining organic solvents and moisture.

2.4 Characterization

2.4.1 Scanning electron microscopy

The fiber morphology was assessed by scanning electron microscopy (SEM; Quanta 200 FEG ESEM, FEI, USA). Prior to examination, samples were sputter-coated with gold under argon to make them electrically conductive. Images were taken at an excitation voltage of 5 kV. The average diameter of the fibers was determined from the SEM images by manual measurements at 100 different points using the ImageJ software (National Institutes of Health, USA).

2.4.2 Thickness of the fiber mat

5 mL of each solution was electrospun onto aluminium foil. A 4 cm diameter circular section was cut from three different locations on the foil with a biopsy punch, and the thickness of each measured using electronic digital Vernier callipers. Data are presented as mean ± S.D. (n=3).

2.4.3 Folding endurance

The brittleness of the fiber mats was quantified in terms of the folding endurance, which is defined as the number of times the mat can be folded at the same place without breaking or cracking (Mundargi et al., 2007). A circular section of 4 cm diameter cut with the biopsy punch was placed in test apparatus built in-house. This is designed to sequentially fold the fiber mat around the central diameter (see Supporting Information, Figure S1). Each fold rotates 180° around the central radius (+90° and -90°). The number of times the mat could be folded until cracks appeared on the fold line was counted (Figure S1). Data from each formulation sample are presented as mean ± S.D. (n=3).

2.4.4 X-ray diffraction

X-ray diffraction patterns were obtained on a MiniFlex 600 Diffractometer (Rigaku, Japan) supplied with Cu Kα radiation (λ = 1.5418 Å) at a voltage of 40 kV and current of 15 mA. Samples were fixed on an aluminium holder and data recorded over the 2θ range between 3 to 45° at a scan speed of 5° min^{-1}.

2.4.5 Differential scanning calorimetry

Differential scanning calorimetry (DSC) studies were conducted using a Q2000 calorimeter (TA instruments, USA). Non-hermetically sealed samples in aluminium pans (Tzero premium pan/lid, TA instruments) were heated over the range 30 to 180 °C for VAL-based materials, or 30 to 220 °C for

formulations containing AB. Experiments were undertaken at a rate of 10 °C min^{-1} and under a nitrogen flow of 50 mL min^{-1}. Data were analysed using the TA instruments Universal Analysis software.

2.4.6 Fourier transform infrared spectroscopy

Infrared (IR) spectra were collected with the aid of a Spectrum 100 spectrometer (PerkinElmer, USA). Samples were studied over the range 4000 to 650 cm^{-1}, with the spectral resolution set at 1 cm^{-1}. 4 scans per sample were recorded.

2.4.7 Drug loading and entrapment efficiency

A high performance liquid chromatography (HPLC) method was developed to simultaneously detect both AB and VAL. This is similar to that previously reported by (Celebier et al., 2010). Samples of 5 ± 0.5 mg were dissolved in 50 mL of methanol then diluted to a final volume of 100 mL with deionised. The resultant solution was sonicated in a water bath for 30 min to ensure complete dissolution.

A calibration curve for AB and VAL was prepared from fresh solutions on the day of the experiment. A quaternary HPLC pump (1200 Infinity Series, Agilent technologies, USA) was used to mix the mobile phase, which comprised 30:35:35 v/v/v phosphate buffered saline (PBS; pH 3.6, 0.01 mol L^{-1}) : acetonitrile : methanol. Adjustment of the PBS pH was undertaken using orthophosphoric acid (85%, HPLC grade, Fisher Scientific, UK) and the solution filtered through a 0.45 µm membrane filters (Millex syringe filter, Merck Millipore, Germany) before use. The stationary phase used was a C18(2) column (00G-4252-E0, Phenomenex Luna, UK). The injected volume was 20 µL, the mobile phase flow rate 1 mL min^{-1}, and the column temperature 40 °C. A UV detector was used for quantification at 240 nm, where AB can be detected at t = 4.9 min and VAL at t = 7.2 min.

The drug loading and entrapment efficiency (%) were calculated from equations (1) and (2). Values are recorded as the mean ± S.D. of 3 independent experiments using a single batch of fibers.

Drug loading (%) = [mass of drug in fiber mat ÷ mass of fiber mat] × 100 (1)

Entrapment efficiency (%) = [mass of drug in fibers ÷ mass of drug in feed solution] × 100 (2)

2.4.8 Wetting assays

A 4 cm diameter circular section of the fiber mat was dropped into an 8 cm Petri dish containing 15 mL of simulated saliva (SS) solution under stirring at 150 rpm. The latter was prepared by mixing 8 g NaCl, 0.19 g KH_2PO_4, and 2.38 g Na_2HPO_4 in 1 L of distilled water. Experiments were performed at room temperature. The wetting and disintegration of the fiber mats were recorded with a high-speed camera (HotShot 1280 CC, NAC Image Technology, Japan) at 500 frames per second.

2.4.9 *In vitro* drug release studies

The intended route of fiber administration is as a fast dissolving oral film. Standard USP methods for dissolution testing do not accurately mimic this, and hence a more realistic *in vitro* release study was employed, similar that reported previously (Illangakoon et al., 2014). 15 mL SS was first pre-warmed to

37.5 ± 2 °C, and transferred into a 8 cm Petri dish held in an oil bath at 37 °C. A sample of the desired formulation (5 ± 0.5 mg) was dropped into the warm SS, and the mixture stirred with a 1 cm magnetic follower at 150 rpm. At predetermined time points a 200 µL sample was taken from the Petri dish for HPLC analysis and replaced with an equal volume of fresh pre-warmed SS, to maintain a total volume of 15 mL. Three independent experiments were carried out and cumulative release percentages are reported as mean ± S.D.

2.4.10 Stability study

The physical form of the components in the electrospun nanofibers was assessed after storage over silica gel in a desiccator for 4 months, using XRD and DSC as detailed above.

3. Results and discussion

3.1 Fiber morphology

SEM images of the nanofibers from all formulations are presented in Figure 1.

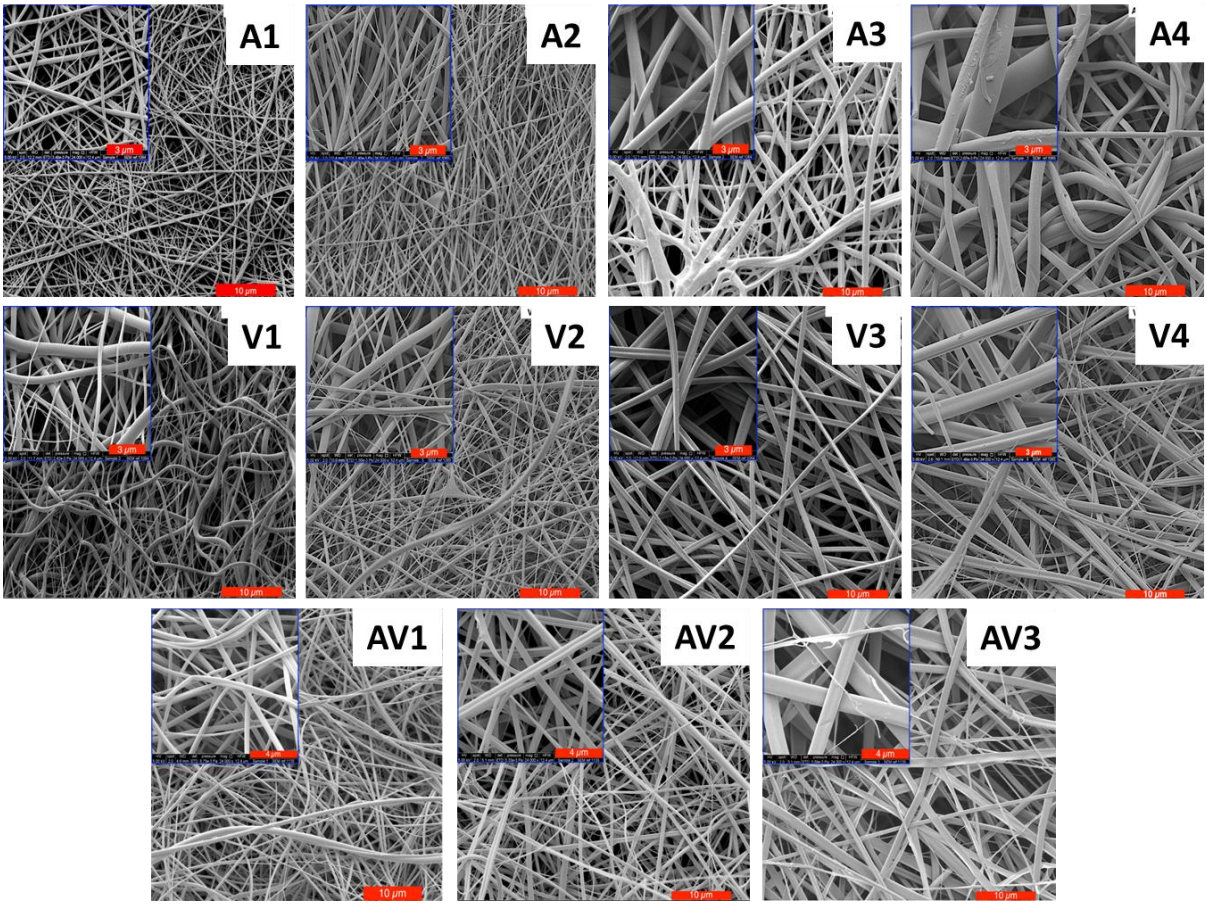

Figure 1: SEM images of the fiber formulations, showing A1 (5% w/w AB); A2 (15% w/w AB); A3 (30% w/w AB); A4 (55% w/w AB); V1 (5% w/w VAL); V2 (15% w/w VAL); V3 (30% w/w VAL); V4 (55% w/w VAL); AV1 (5% w/w AB, 5% w/w VAL); AV2 (10% w/w AB, 10% w/w VAL); and, AV3 (30% w/w AB, 30% w/w VAL). Scale bars: main images 10 µm; insets for A1 – A4 and V1 – V4 3 µm; insets for AV1 – AV3 4 µm.

The images show that fibers have formed in all cases. The AB-loaded fibers A1 to A4 all have smooth cylindrical morphologies, with some small particles visible in A4. In contrast, the VAL-containing fibers V1 to V4 and AV1 to AV3 change from cylindrical shapes to flattened ribbon-like fibers as the drug loading increases. This may be a result of the solution having high viscosity at the higher loadings, leading to incomplete evaporation during electrospinning. Subsequent evaporation of the residual solvent during storage leads to the formation of flattened fibers (Koski et al., 2004). Some precipitation of the drug was also noted during spinning with the higher concentration VAL-containing solutions (V4, AV3; data not shown). Regardless of this, no drug crystals can be seen on the fiber surfaces.

The diameters of the fibers are detailed in Table 2. When the drug loading percentage was increased, the fiber diameter rises. This is as expected, since an increase in drug content results in an increase in the amount of mass expelled from the spinneret per unit time, and is in good agreement with literature data on the electrospinning of PVP fibers loaded (Illangakoon et al., 2014; Lopez et al., 2014; Yu et al., 2009)

3.2 Mat thickness

The thickness of the fiber mats was measured for 4 cm circular cuts taken from different locations with each formulation (Table 2). The data show an increase in thickness for formulation A0 to A4 as the AB loading rises from 0 to 55%. In contrast, with V0 – V4 the thickness of the mat decreases as the loading increases. In the combined-drug AV formulations the average mat thickness again increases with the drug content. These changes in thickness may be to the different shapes of the fibers in each formulation. The AB and AB/VAL fibers are generally all cylindrical, except for AV3. In contrast, there is a move to flat ribbon-like fibers with an increasing drug loading in the VAL systems (see Figure 1). Inside the fiber mat, the cylindrical fibers occupy a greater vertical bulk compared to the ribbon-like fibers. When increasing the loading of AB from A0 to A4 the fibers become thicker, causing the mat to thicken in turn. In contrast, increasing the VAL loading from V0 to V4 led to more flattened fibers accumulating and a thinner mat. A balance of these factors is operational in the AV systems, resulting overall in a small increase in thickness with the drug loading.

For oral fast dissolving formulations, the optimised film thickness range has been proposed to be between 20-500 µm (Bala et al., 2013). The results in Table 2 show that the mats prepared in this work fall within this range, and suggests there is the flexibility to increase the collection time to produce thicker mats with a larger mass of drug incorporated if required.

3.3 Folding endurance

Folding endurance is mechanical property used to characterize the ability of thin films to resist cracking or breaking upon packaging, storing and patient usage (Vuddanda et al., 2016). Folding endurance results are reported in Table 2. The folding endurance of the fibers decreases with a rising drug loading, as a result of the fibers becoming more brittle and mechanically weaker (Bölgen et al., 2005). However, all the values are generally high, and compare favourably with the literature (Illangakoon et al., 2014).

This indicates that all the formulations prepared have appropriate mechanical properties to find application as oral films.

Table 2: Characterising data for the fiber mats. Diameters are calculated from 100 measurements in ImageJ. Thickness and folding endurance data are from three repeat experiments. All data are presented as mean ±S.D.

Formulation	Fiber diameter (nm)	Thickness (µm)	Folding endurance (number of folds)
Blank PVP fibers	--	320 ± 26	61 ± 2
A1	344 ± 70	338 ± 50	54 ± 15
A2	474 ± 86	340 ± 30	51 ± 10
A3	880 ± 294	352 ± 60	35 ± 4
A4	1230 ± 400	450 ± 100	30 ± 4
V1	724 ± 120	330 ± 51	80 ± 1
V2	741 ± 107	206 ± 20	72 ± 16
V3	882 ± 127	146 ± 25	46 ± 11
V4	909 ± 384	150 ± 10	17 ± 6
AV1	461 ± 72	160 ± 10	80 ± 34
AV2	737 ± 154	210 ± 10	36 ± 4
AV3	1270 ± 278	260 ± 20	17 ± 9

3.4 Physical form

The physical form of the drug components in the nanofibers was examined by XRD and DSC. XRD results are given in Figure 3. The AB pattern displays a series of sharp Bragg reflections consistent with its anhydrous form (Koradia et al., 2010). VAL displays some reflections, but these are weak and broad. It is known that it is challenging to prepare highly crystalline VAL, and commercial materials show poor crystallinity (Wang et al., 2013). These observations are therefore all consistent with the literature. In contrast, PVP is clearly amorphous with only broad haloes in its diffraction pattern.

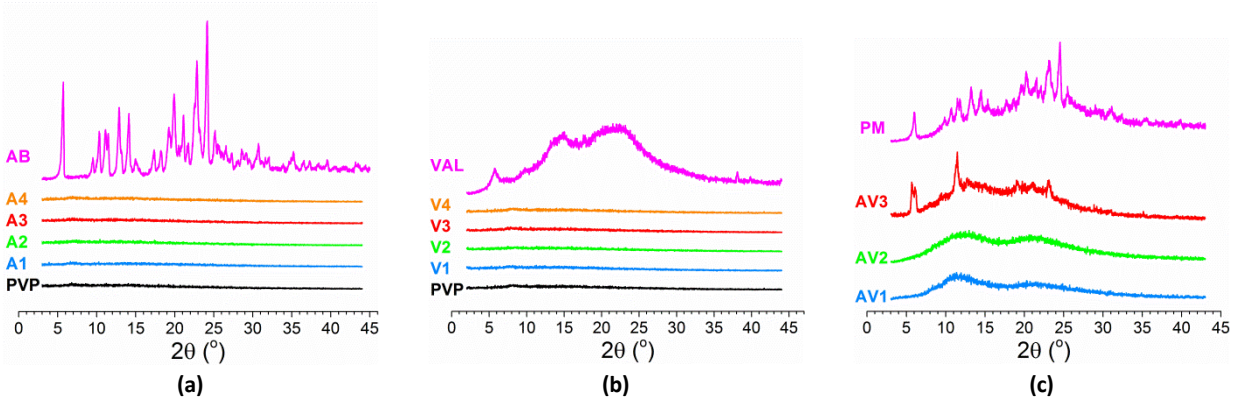

Figure 2: XRD diffraction patterns of the nanofiber formulations and raw materials. (a) AB-loaded fibers; (b) VAL-loaded fibers; and (c) AB/VAL dual drug systems. PM: physical mixture (30% AB / 30% VAL / 40% PVP by mass).

All the electrospun fibers loaded with AB (Figure 2(a)) and VAL (Figure 2(b)) show no Bragg reflections, demonstrating that the fibers comprise amorphous solid dispersions. In the patterns of AV1 and AV2, the characteristic reflections of AB and VAL have again disappeared, consistent with the formation of an amorphous system (Figure 2(c)). The formation of amorphous solid dispersions after electrospinning has

been reported by a large number of studies in the literature (Jin et al., 2016; Lopez et al., 2014; Zamani et al., 2013), and arises due to the rapid evaporation of solvent induced by the process. This typically prevents the organisation of molecules into crystalline lattices, and leads to the propagation of the disordered arrangement of molecules in the initial solution into the solid products.

In formulation AV3, however, some characteristic reflections of AB can be seen in the diffraction pattern (Figure 2(c)), and the formulation's pattern is similar to that of a physical mixture (PM) of AB, VAL and PVP in the same ratios. This indicates that some of the drug in AV3 is crystalline. This is a result of the high drug loading in the AV3 system, and is consistent with the precipitates seen to form in the syringe during electrospinning.

The DSC thermograms (Figure 3) concur well with the findings from XRD. The raw materials show sharp melting endothermic peaks for AB at around 206 °C, and for VAL at 103 °C. These are close to the literature value of 199 – 201 °C recorded for AB (http://www.chemicalbook.com/ChemicalProductProperty_US_CB4127875.aspx), but rather distant from the 116 – 117 °C expected for VAL (https://pubchem.ncbi.nlm.nih.gov/compound/valsartan#section=Top). The latter difference can be ascribed to the poor crystallinity of the VAL sample procured for this work. PVP presents a broad endotherm that starts at around 50 °C and finishes at *ca.* 135 °C, as a result of water loss. There are no melting events visible, as expected since PVP is widely known to be amorphous.

The thermograms of the electrospun fibers show broad dehydration endotherms between around 30 and 130 °C, but in most cases there are no melting endothermic peaks visible. The loss of characteristic endotherms for A1 to A3, V1 to V4, AV1 and AV2 means that the drug in the polymer matrix is present in the amorphous form in these fibers (Vigh et al., 2013), in agreement with the XRD data above. There are two exceptions, however. In formulation A4, a small endothermic peak appears at 201 °C, which can be ascribed to AB melting (Silva et al., 2014). Given that XRD does not show any evidence of crystalline material being present in A4, it is thought that recrystallisation must have occurred upon heating in the DSC experiment. There is also a small endotherm at approximately 195 °C in the AV3 formulation, indicating some crystalline AB is melting. This is again consistent with the XRD data, which revealed the presence of some crystalline drug at room temperature.

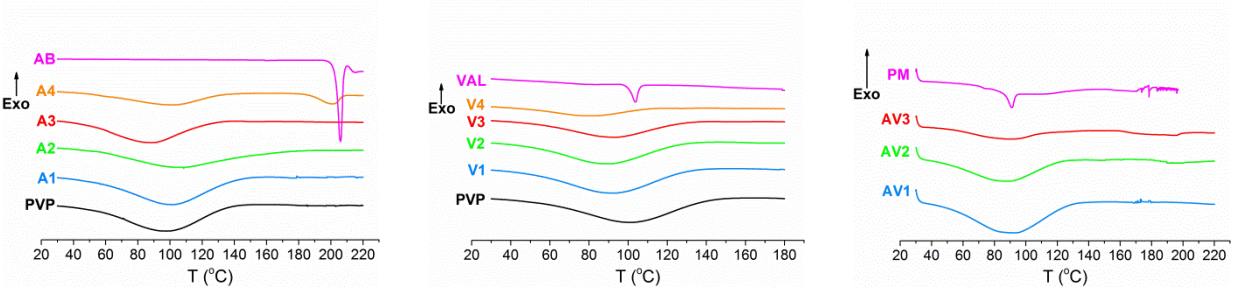

Figure 3: Differential scanning calorimetry data for (a) AB; (b) VAL; and (c) the FDC fibers. PM: physical mixture (30% AB / 30% VAL / 40% PVP by mass).

3.5 Infrared spectroscopy

IR spectra were collected to investigate the drug-polymer interactions and help understand the compatibility of the APIs with the polymer in the fibers. Compatibility is essential for producing high quality and stable nanocomposites, because solid phase separation might occur if the API is not compatible with the polymer. The molecular structures of AB and VAL are shown in Figure 4(a). Full-length IR spectra can be found in Figure S2, while enlargements of the carboxylate region are given in Figure 4(b)-(d).

The IR spectrum of AB shows characteristic C=O stretches at 1697cm^{-1} and 1673 cm^{-1}, and a sharp peak at 1089 cm^{-1} with a shoulder at 1114 cm^{-1} from the C-O-C asymmetric stretch. Other peaks are present at 1048 cm^{-1} (NH_3 wagging), at 869 cm^{-1} (-C-O in plane bending), and at 753 cm^{-1}, 728 cm^{-1}, and 689 cm^{-1} for (N-H vibrations). The IR spectrum of VAL has characteristic peaks at 3300 cm^{-1} (O-H, and N-H stretching vibrations), and at 2963 cm^{-1} (aromatic CH_2 stretching vibration), 1730 cm^{-1} (C=O carbonyl vibration), 1603 cm^{-1} (N-C=O amide carbonyl stretching), and 1451 and 1470 cm^{-1} (aromatic C=C vibrations). Pure PVP shows bands from 3650 – 3050 cm^{1} (O-H stretches from adsorbed water), 2840 – 3010 cm^{1} (C-H stretches), 1660 cm^{1} (C=O) and 1290 cm^{1} (C-N stretch).

The spectra of the electrospun fibers show significant changes from the raw materials. These are most noticeable in the spectra of the highest drug loading formulations. The AB C=O stretches at 1697 cm^{-1} and 1673 cm^{-1} have both merged into the PVP C=O peak at 1660 cm^{-1}. Similarly, the C-O-C vibration at 1114 cm^{-1} in AB shifts to 1123 cm^{-1} in the fibers. In the spectrum of V4, the VAL peaks present at 1603 cm^{-1} (N-C=O amide carbonyl stretching) and 1470 cm^{-1} (aromatic C=C) for the pure drug are shifted to 1637 cm^{-1} and 1461 cm^{-1}. Similar findings are noted for the FDC fibers.

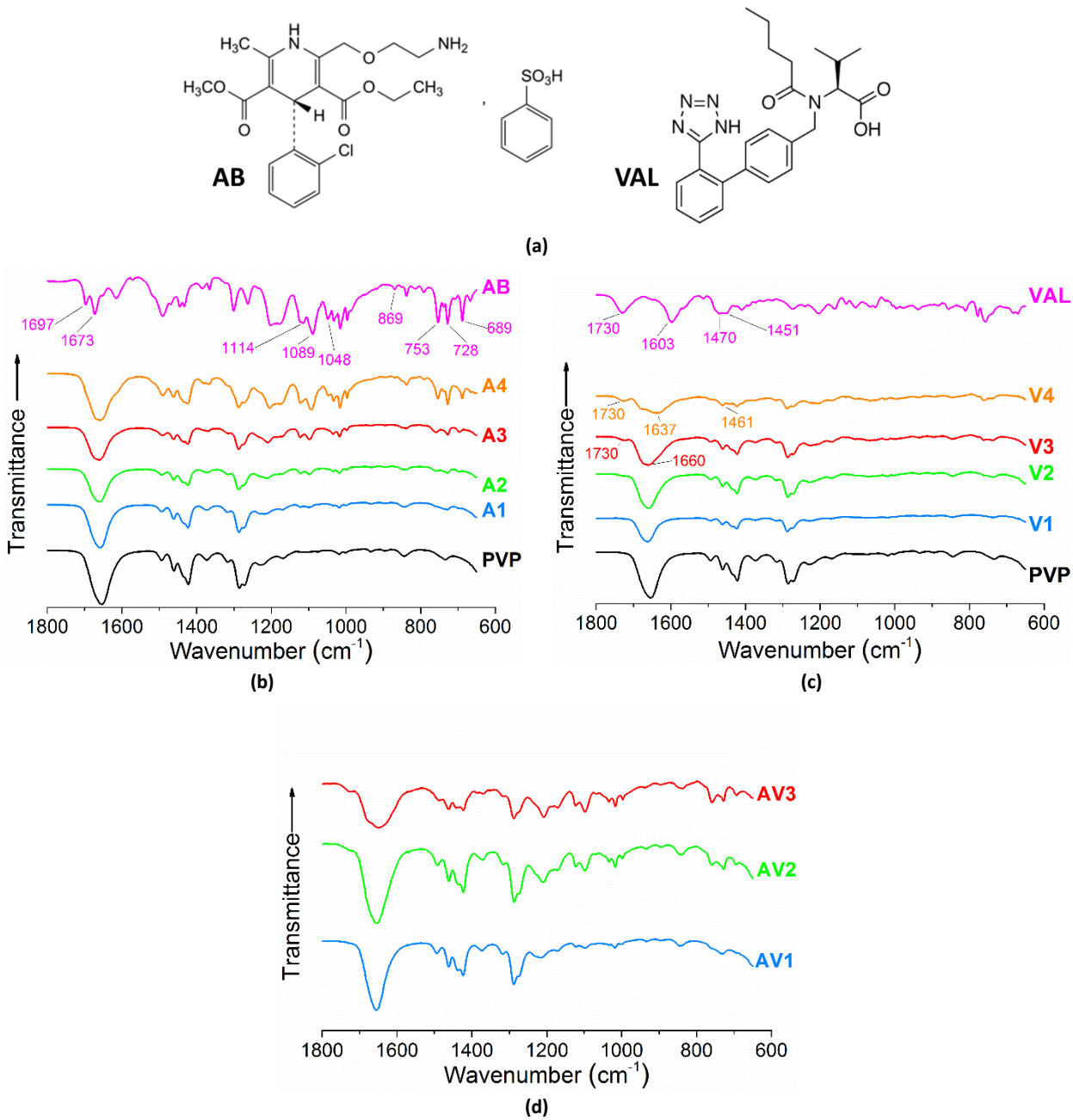

343 **Figure 4.** (a) The chemical structures of AB and VAL, together with IR spectra for the (b) AB; (c) VAL; and, (d) FDC fibers. PM: A
344 physical mixture of AB, VAL, and PVP.
345
346 All these observations indicate the formation of intermolecular bonds between the drugs and PVP (Chen
347 et al., 2008). The formation of interactions such as hydrogen bonding (between e.g. N-H and O-H groups
348 in AB and VAL and the C=O groups of PVP), van der Waals interactions, and other secondary interactions
349 such hydrophobic interactions (between the aromatic groups of the drugs and polymer), should lead to
350 good compatibility between the components in the fiber mat (Wu et al., 2015) and aid the long term
351 stability of the formulations (Mukherjee et al., 2005).
352

3.6 Drug loading and entrapment efficiency

The drug loading and encapsulation efficiencies were determined by HPLC (see Table 4). All the entrapment efficiencies are ≥ 85%, with most very close to 100%. This is as expected, since there is minimal scope for loss of material in the electrospinning experiment unless there is precipitation in the syringe. In some cases, it can be seen that the EE values are > 100%; we ascribe this to a degree of batch-to-batch variability in the formulations, particularly in terms of the amount of water present (PVP is hygroscopic, and so will absorb water).

Table 4. The drug loadings and encapsulation efficiencies (EE) of the fibers. Data are reported as mean ± S.D. from three experiments.

Formulation	AB loading (% w/w)	AB EE (% w/w)	VAL loading (% w/w)	VAL EE (%)
A1	5.3 ± 0.3	107.3 ± 5.8	-	-
A2	14.4 ± 0.8	96.2 ± 5.4	-	-
A3	26.0 ± 3.4	86.8 ± 11.2	-	-
A4	56.6 ± 1.1	102.9 ± 2.1	-	-
V1	-	-	4.5 ± 0.2	90.0 ± 0.5
V2	-	-	14.8 ± 0.6	98.6 ± 3.9
V3	-	-	29.7 ± 0.3	99.0 ± 0.9
V4	-	-	54.7 ± 2.3	99.5 ± 4.2
AV1	5.4 ± 0.3	108.9 ± 5.0	5.48 ± 0.2	109.7 ± 4.0
AV2	14.6 ± 0.3	97.1 ± 2.3	14.99 ± 0.5	99.9 ± 3.4
AV3	27.0 ± 0.4	90.0 ± 1.4	31.32 ± 0.7	104.4 ± 2.4

3.7 Wetting assays

In this study a minimal volume of SS was used to simulate the amount of moisture in the mouth and the time taken for disintegration determined for A1 and A3 using a high speed camera (Figure 5). Complete disintegration is observed in < 1 s for A1, and < 3 s for A3. This is slightly slower than previously reported for PVP-based fibers (Illangakoon et al., 2014), but nevertheless very promising for fast dissolving films. Results from other studies on oral fast dissolving formulations reported a range of disintegration times between 8 and 20 seconds (Cilurzo et al., 2011; Yu et al., 2009).

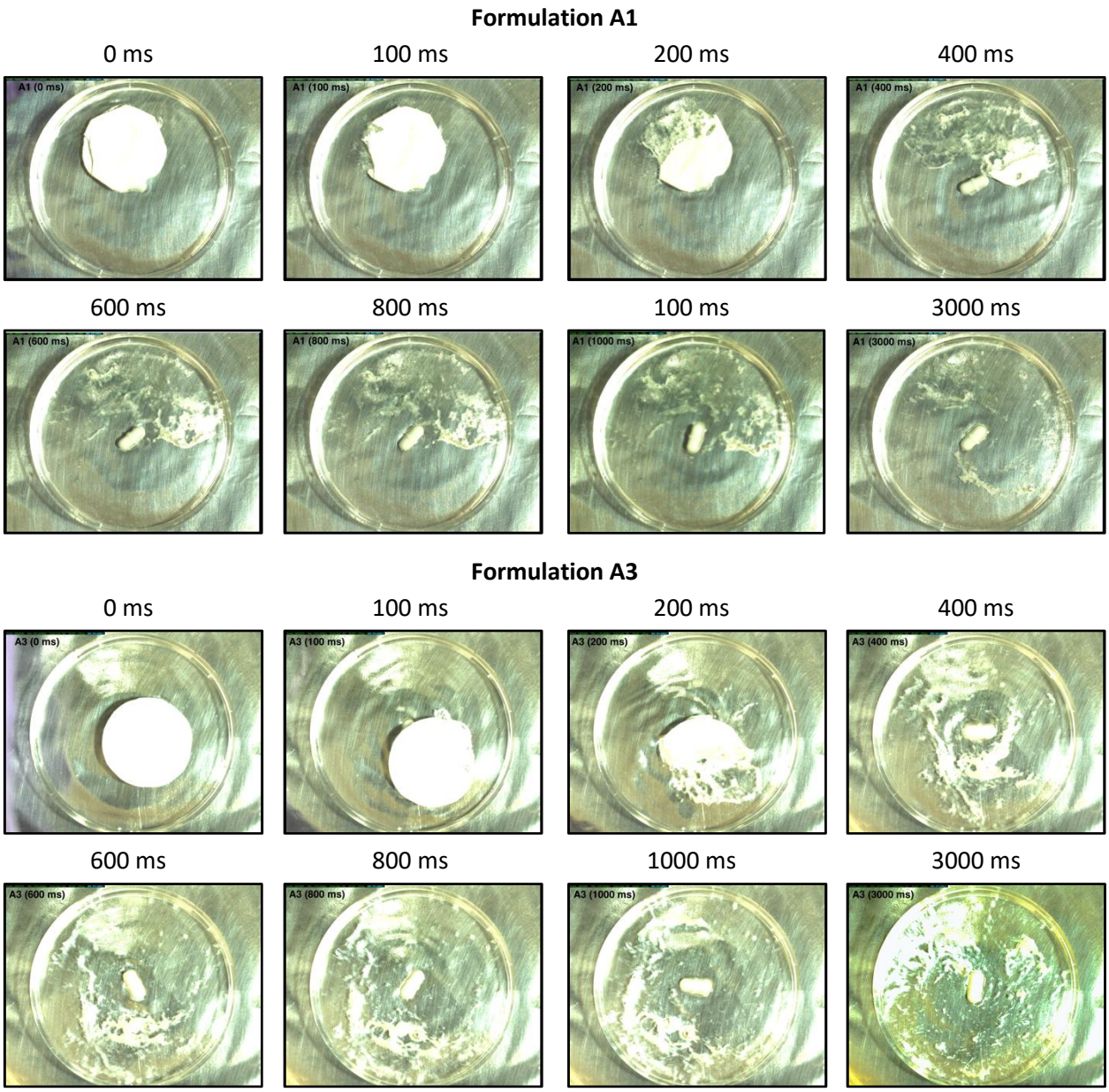

Figure 5: High speed camera images of the disintegration of A1 and A3 in simulated saliva.

3.8 In vitro *drug release*

In vitro dissolution tests were carried out in artificial simulated saliva. The results are given in Figure 6. In some cases release percentages a little over 100% are observed; this can be attributed to a degree of batch-to-batch variability in the formulations. Release of AB from all its single-drug fibers was very rapid: over 90% of the loading was released after 120 s for A1, A2 and A3, and after 270 s with A4 (see Figure 6(a)). Similar findings were obtained in a study by (Yu et al., 2009) on PVP electrospun fibers loaded) with ibuprofen, where an increase in drug loading also extended the release time.

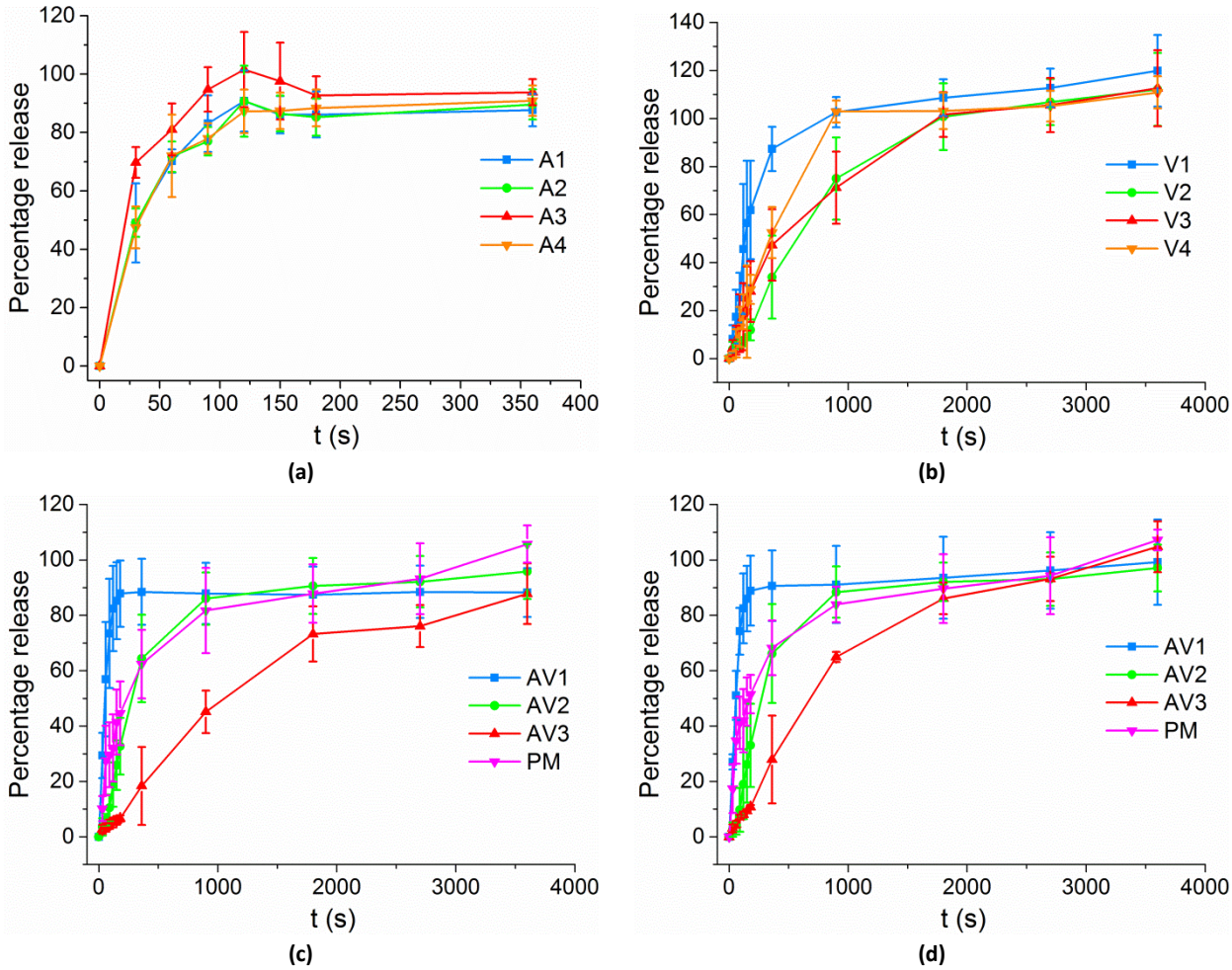

Figure 6: *In vitro* dissolution profiles showing (a) release of AB from A1 to A4; (b) release of VAL from V1 to V4; (c) release of AB from the FDC fiber mats; and, (d) release of VAL from FDC fibers. PM: physical mixture (30% AB / 30% VAL / 40% PVP by mass).

The release of VAL from V1 – V4 was much slower, however (Figure 6(b)). Drug release from V1 reached 90% only after 370 s, slightly over 6 min. The other materials were even slower to release, with V4 not attaining 90% release until some 24 min after the start of the experiment. The key factor controlling release from V1 is the presence of 95% w/w PVP in the fibers, which enhances the disintegration of the fibers and the dissolving of VAL into solution. As the VAL loading increases, the PVP content in the fibers declines, and thus disintegration and dissolution slow down. A similar lengthening of the release time is noted with AB, but this is much less significant because AB is a salt and thus has substantially higher solubility than VAL.

In the combined-drug AV formulations, from each FDC the release profiles of both APIs (see Figure 6(c) and (d)) are very similar. With AV1, fast release of both drugs is seen, and 360 s into the experiment release reaches 88 ± 12% for AB, and 90 ± 13% for VAL. This presumably arises because of the high content of the hydrophilic polymer PVP and the molecular dispersion of AB and VAL in it. In addition to VAL AV1 contains PVP and also highly soluble AB; the presence of these two hydrophilic entities (cf just PVP and VAL in V1) accelerated the disintegration of the formulation and freeing of VAL into solution.

Formulation AV1 is potentially therefore a good choice for fabricating fast dissolving FDC formulation with an immediate release of APIs into the oral cavity.

As for the single-drug fibers, an increasing drug loading leads to a slowing in the rate of drug dissolution, however. In AV2, 90% release of AB was attained only after 1800 s (30 min), and 90% of the VAL content after 900 s. For AV3, the 90% release times > 3600 s for AB and 2190 s for VAL. All these times are much too long for an effective oral film, and cannot be said to be fast dissolving. Indeed, AV3 dissolves more slowly than an analogous physical mixture of the drugs and PVP (see Figure 7(c) and (d)). The reasons behind this are not completely clear, but it is evident from the XRD data (Figure 2(c)) that AV3 contains crystalline material. This, coupled with drug/polymer interactions and a relatively slow disentanglement of the PVP polymer molecules when the formulation is added to water, is expected to be responsible for slowing the rate of drug release over the physical mixture.

3.9 Stability study

Since amorphous materials will seek to relax to a crystalline state over time, the storage stability of the fibers was explored. XRD data were recorded on fibers which had been stored in a desiccator for 4 months (see Figure 7). The diffraction data clearly show the bulk of the formulations remain amorphous over this time, and distinct Bragg reflections can only be seen for A4 and AV3. In both of these cases there is very clear evidence for the recrystallization of AB. VAL recrystallization cannot be ascertained, but this is not surprising since VAL is known to be poorly crystalline, and also the presence of ions in AB will encourage more rapid reversion to an ordered form. It appears that phase separation may be starting to occur after 4 months' ageing for A4 and AV3, a phenomenon also noticed by Lopez et al., (2014) upon the aging of PVP-based fibers.

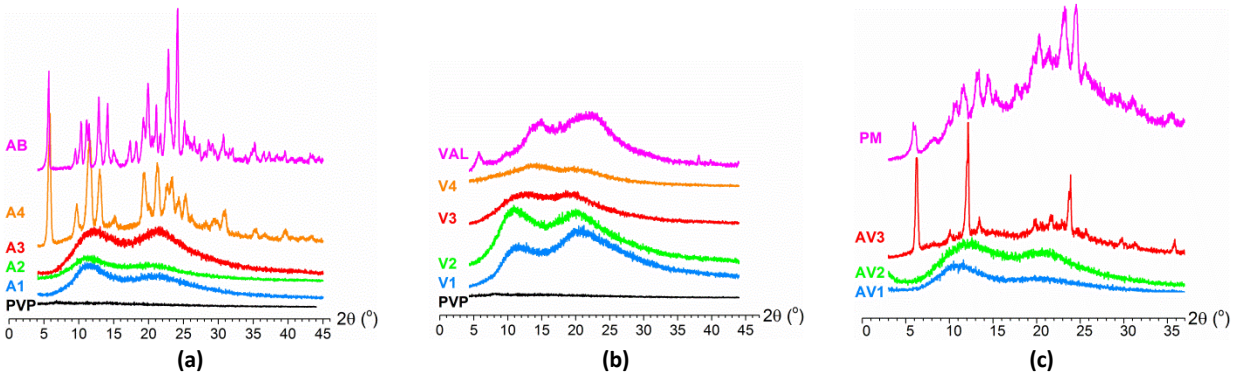

Figure 7: Physical characterisation data obtained on aged materials. XRD data are shown for the (a) AB; (b) VAL; and, (c) FDC fibers.

Overall, it is clear from this study that electrospun nanofibers can be loaded with multiple drugs to provide rapid release in conditions representative of the mouth, and that at lower doses the fibers are stable upon storage for at least four months. They thus offer a smart drug delivery platform for treating co-morbidities in the elderly population. The drug release profile was found to be dependent on the drug loading, and these results will be helpful to guide future studies aiming to fabricate immediate release FDC formulations for co-morbidities. The fast dissolving feature of the electrospun fiber systems

reported here is also expected to lead to high acceptability by patients with swallowing difficulties, and hence to lead to higher adherence.

4. Conclusions

The aim of this study was to utilize electrospinning to prepare FDC fast-dissolving drug delivery systems. We were able to develop nanofibers with drug loadings between 5% and 55% w/w. Two types of formulation were made, loaded either with a single drug (valsartan or amlodipine besylate), or both. Characterisation the fibers by scanning electron microscopy showed most to be cylindrical with smooth surfaces, but with a tendency to flatten with increased valsartan loadings. The fiber mats obtained had thicknesses between 146 and 450 µm, and most showed acceptable folding endurance except at very high drug loadings. R studies revealed intermolecular interactions between AB, VAL, and the polymer PVP in the composite material, and X-ray diffraction and differential scanning calorimetry showed the majority of the formulations to comprise amorphous solid dispersions. Entrapment efficiencies were greater than 85% in all cases. The fiber mats wet and disintegrate in under 3 s, indicating they have promise as oral fast-dissolving films. *In vitro* dissolution studies demonstrated that the amlodipine besylate-loaded fibers had fast release profiles freeing 90% of their drug cargo within 120 s with loadings of 30% w/w and below, or 360 s from s 55% w/w formulation. In contrast, the valsartan formulations released their drug cargo much more slowly, with even 5% w/w fibers only reaching 90% release at *ca.* 360 s, while the 55% w/w fiber required 24 min to reach this point. In the fixed dose combination fibers, the drug release profile varied markedly with the drug loading. 90% release of both drugs was reached within 360 s was achieved when the loading of each was 5% w/w, but the rate declines rapidly as more drug is added. Except for those with the highest drug loadings, the fibers remain amorphous for at least 4 months' storage in a dessicator.

5. Acknowledgements

The authors thank the Umm AlQura University (Kingdom of Saudi Arabia) for provision of a scholarship to HB. We also gratefully acknowledge Mr Dave McCarthy and Mrs Kate Keen for assistance with obtaining SEM images, and Dr Asma Buanz for guidance on DSC experiments.

6. References

Adeli, E., 2015. Irbesartan-loaded electrospun nanofibers-based PVP K90 for the drug dissolution improvement: Fabrication, in vitro performance assessment, and in vivo evaluation. J. Appl. Polym. Sci. 132, 42212.

Bala, R., Pawar, P., Khanna, S., Arora, S., 2013. Orally dissolving strips: A new approach to oral drug delivery system. Int. J. Pharm. Investig. 3, 67-76.

Bangalore, S., Kamalakkannan, G., Parkar, S., Messerli, F.H., 2007. Fixed-dose combinations improve medication compliance: a meta-analysis. Am. J. Med. 120, 713-719.

Bölgen, N., Menceloğlu, Y.Z., Acatay, K., Vargel, İ., Pişkin, E., 2005. In vitro and in vivo degradation of non-woven materials made of poly(ε-caprolactone) nanofibers prepared by electrospinning under different conditions. J. Biomed. Sci. Polym. Ed. 16, 1537-1555.

Celebier, M., Kaynak, M.S., Altınöz, S., Sahin, S., 2010. HPLC method development for the simultaneous analysis of amlodipine and valsartan in combined dosage forms and in vitro dissolution studies. Brazil. J. Pharm. Sci 46, 761-768.

Chen, J., Wang, X., Zhang, W., Yu, S., Fan, J., Cheng, B., Yang, X., Pan, W., 2016. A novel application of electrospinning technique in sublingual membrane: characterization, permeation and in vivo study. Drug. Dev. Ind. Pharm. 42, 1365-1374.

Chen, Z., Mo, X., He, C., Wang, H., 2008. Intermolecular interactions in electrospun collagen–chitosan complex nanofibers. Carbohydr. Polym. 72, 410-418.

Cilurzo, F., Cupone, I.E., Minghetti, P., Buratti, S., Gennari, C.G., Montanari, L., 2011. Diclofenac fast-dissolving film: suppression of bitterness by a taste-sensing system. Drug Dev. Ind. Pharm. 37, 252-259.

Desai, D., Wang, J., Wen, H., Li, X., Timmins, P., 2013. Formulation design, challenges, and development considerations for fixed dose combination (FDC) of oral solid dosage forms. Pharm. Dev. Technol. 18, 1265-1276.

European Medicines Agency, 2017. Reflection paper on the pharmaceutical development of medicines for use in the older population.

Fulton, M.M., Allen, E., 2005. Polypharmacy in the elderly: a literature review. J. Am. Acad. Nurse Pract. 17, 123-132.

Gorard, D.A., 2006. Escalating polypharmacy. QJM 99, 797-800.

http://www.chemicalbook.com/ChemicalProductProperty_US_CB4127875.aspx.

https://pubchem.ncbi.nlm.nih.gov/compound/valsartan#section=Top.

Hughes, C.M., 2004. Medication non-adherence in the elderly. Drugs & Aging 21, 793-811.

Illangakoon, U.E., Gill, H., Shearman, G.C., Parhizkar, M., Mahalingam, S., Chatterton, N.P., Williams, G.R., 2014. Fast dissolving paracetamol/caffeine nanofibers prepared by electrospinning. Int. J. Pharm. 477, 369-379.

Jimmy, B., Jose, J., 2011. Patient medication adherence: measures in daily practice. Oman Med. J. 26, 155-159.

Jin, M., Yu, D.G., Geraldes, C.F., Williams, G.R., Bligh, S.W., 2016. Theranostic fibers for simultaneous imaging and drug delivery. Mol. Pharm. 13, 2457-2465.

Khaled, S.A., Burley, J.C., Alexander, M.R., Yang, J., Roberts, C.J., 2015. 3D printing of five-in-one dose combination polypill with defined immediate and sustained release profiles. J. Controlled Release 217, 308-314.

Koradia, V., Lopez de Diego, H., Frydenvang, K., Ringkjøbing-Elema, K., Müllertz, A., Bond, A.D., Rantanen, J., 2010. Solid forms of amlodipine besylate: Physicochemical, structural, and thermodynamic characterization. Cryst. Growth Des. 10, 5279-5290.

Koski, A., Yim, K., Shivkumar, S., 2004. Effect of molecular weight on fibrous PVA produced by electrospinning. Mater. Lett. 58, 493–497.

Li, X., Kanjwal, M.A., Lin, L., Chronakis, I.S., 2013a. Electrospun polyvinyl-alcohol nanofibers as oral fast-dissolving delivery system of caffeine and riboflavin. Colloids Surf. B 103, 182-188.

Li, X., Lin, L., Zhu, Y., Liu, W., Yu, T., Ge, M., 2013b. Preparation of ultrafine fast-dissolving cholecalciferol-loaded poly(vinyl pyrrolidone) fiber mats via electrospinning. Polym. Composite. 34, 282-287.

Liu, F., Ranmal, S., Batchelor, H.K., Orlu-Gul, M., Ernest, T.B., Thomas, I.W., Flanagan, T., Tuleu, C., 2014. Patient-centred pharmaceutical design to improve acceptability of medicines: similarities and differences in paediatric and geriatric populations. Drugs 74, 1871-1889.

519 Lopez, F.L., Shearman, G.C., Gaisford, S., Williams, G.R., 2014. Amorphous formulations of indomethacin
520 and griseofulvin prepared by electrospinning. Mol. Pharm. 11, 4327-4338.
521 Mitra, A., Wu, Y., 2012. Challenges and opportunities in achieving bioequivalence for fixed-dose
522 combination products. AAPS J. 14, 646-655.
523 Mukherjee, B., Mahapatra, S., Gupta, R., Patra, B., Tiwari, A., Arora, P., 2005. A comparison between
524 povidone-ethylcellulose and povidone-eudragit transdermal dexamethasone matrix patches based on in
525 vitro skin permeation. Eur. J. Pharm. Biopharm. 59, 475-483.
526 Mundargi, R.C., Patil, S.A., Agnihotri, S.A., Aminabhavi, T.M., 2007. Evaluation and controlled release
527 characteristics of modified xanthan films for transdermal delivery of atenolol. Drug Dev. Ind. Pharm. 33,
528 79-90.
529 Nagy, Z.K., Nyul, K., Wagner, I., Molnar, K., Marosi, G., 2010. Electrospun water soluble polymer mat for
530 ultrafast release of Donepezil HCl. Express Polym. Lett. 4, 763-772.
531 Plosker, G.L., Robinson, D.M., 2008. Amlodipine/Valsartan: fixed-dose combination in hypertension.
532 Drugs 68, 373-381.
533 Seager, H., 1998. Drug-delivery products and the Zydis fast-dissolving dosage form. J. Pharm. Pharmacol.
534 50, 375-382.
535 Silva, A.C.M., Gálico, D.A., Guerra, R.B., Perpétuo, G.L., Legendre, A.O., Rinaldo, D., Bannach, G., 2014.
536 Thermal stability and thermal decomposition of the antihypertensive drug amlodipine besylate. J.
537 Therm. Anal. Calorim. 120, 889-892.
538 Vigh, T., Horvathova, T., Balogh, A., Soti, P.L., Dravavolgyi, G., Nagy, Z.K., Marosi, G., 2013. Polymer-free
539 and polyvinylpirrolidone-based electrospun solid dosage forms for drug dissolution enhancement. Eur. J.
540 Pharm. Sci. 49, 595-602.
541 Vuddanda, P.R., Mathew, A.P., Velaga, S., 2016. Electrospun nanofiber mats for ultrafast release of
542 ondansetron. React. Funct. Polym. 99, 65-72.
543 Wang, J.-R., Wang, X., Lu, L., Mei, X., 2013. Highly crystalline forms of valsartan with superior
544 physicochemical stability. Cryst. Growth Des. 13, 3261-3269.
545 Williams, G.R., Chatterton, N.P., Nazir, T., Yu, D.-G., Zhu, L.-M., Branford-White, C.J., 2012. Electrospun
546 nanofibers in drug delivery: recent developments and perspectives. Therap. Deliv. 3, 515-533.
547 Wu, Y.-H., Yu, D.-G., Li, X.-Y., Diao, A.-H., Illangakoon, U.E., Williams, G.R., 2015. Fast-dissolving sweet
548 sedative nanofiber membranes. J. Mater. Sci. 50, 3604-3613.
549 Yu, D.-G., Branford-White, C., Shen, X.-X., Zhang, X.-F., Zhu, L.-M., 2010. Solid dispersions of ketoprofen
550 in drug-loaded electrospun nanofibers. J. Dispersion Sci. Technol. 31, 902-908.
551 Yu, D.G., Shen, X.X., Branford-White, C., White, K., Zhu, L.M., Bligh, S.W., 2009. Oral fast-dissolving drug
552 delivery membranes prepared from electrospun polyvinylpyrrolidone ultrafine fibers. Nanotechnol. 20,
553 055104.
554 Zamani, M., Prabhakaran, M.P., Ramakrishna, S., 2013. Advances in drug delivery via electrospun and
555 electrosprayed nanomaterials. Int. J. Nanomedicine 8, 2997-3017.
556